

PUBLISHED BY

# INTECH

open science | open minds

World's largest Science,  
Technology & Medicine  
Open Access book publisher



**3,100+**  
OPEN ACCESS BOOKS



**103,000+**  
INTERNATIONAL  
AUTHORS AND EDITORS



**102+ MILLION**  
DOWNLOADS



**BOOKS**  
DELIVERED TO  
151 COUNTRIES

AUTHORS AMONG

**TOP 1%**  
MOST CITED SCIENTIST



**12.2%**  
AUTHORS AND EDITORS  
FROM TOP 500 UNIVERSITIES



Selection of our books indexed in the  
Book Citation Index in Web of Science™  
Core Collection (BKCI)

**WEB OF SCIENCE™**

Chapter from the book *Artificial Neural Networks - Application*

Downloaded from: <http://www.intechopen.com/books/artificial-neural-networks-application>

Interested in publishing with InTechOpen?  
Contact us at [book.department@intechopen.com](mailto:book.department@intechopen.com)

# Applications of Neural Networks in Advanced Oxidative Process

Messias Borges Silva, Oswaldo Luiz Cobra Guimarães, Adriano Francisco Siqueira, Hécio José Izário Filho, Darcy Nunes Villela Filho, Henrique Otávio Queiroz de Aquino, Ivy dos Santos Oliveira and Carlos Roberto de Oliveira Almeida  
*University of São Paulo – School of Engineering of Lorena  
Brazil*

## 1. Introduction

This chapter has the objective of presenting four studies involving neural networks in the area of advanced oxidative process. Advanced Oxidative Processes area based on the generation and reaction of hydroxyl radicals. Because they are not selective and it possesses a high oxidizing power are able to degrade organic contaminants.

Mathematical modeling of chemical process is often addressed in photocatalytic function of some parameters that are inherent in the process, such as the geometry of a reactor or characteristics of the compound to be worked, such as solubility and spectral characteristics of organic compounds. By moving the geometry of the reactor, moves through the proposed model. When they moved the reagents, changes completely the kinetics of the reactions involved and consequently the reactor performance.

The process of decolorization and degradation of organic compounds may involve, according to criteria adopted modeling, a series of reactions kinetics. The photocatalytic process modeling involves the solution to a complex set of equations of energy (radiation), the mass balance, momentum and heat, being a difficult process description. The performance of a photoreactor is strongly influenced by many physical-chemical interaction occurring between these variables. Conventional modeling techniques can produce models not appropriate.

This sense, neural modeling, empirical, presents itself as alternative to the traditional model, because it is based on mathematical equation. Based on the study of behavioral characteristics of the sets of input and output of the process of discoloration and degradation of organic compounds, possessing the ability to "learn" the behavior of linear or nonlinear experimental data. Through this "learning" may provide the optimization of the action of hydroxyl radical oxidation.

Are presented four applications involving neural networks modeling.

- a. Neural approximation of the reduction of cod effluents from the manufacturing of polyesters trough photo-fenton proces/ ozonization
- b. Hybrid neural model for decoloration by UV/ H<sub>2</sub>O<sub>2</sub> involving process variables and structural parameters characteristics to azo dyes

- c. Optimization of the AZO dyes decoloration process through neural networks:
  - Determination of the H<sub>2</sub>O<sub>2</sub> addition critical point
- d. Decoloration process modeling by neural network

## 2. Artificial Neural Networks

A neural network is formed by processing elements (neurons) interconnected with the bordering neurons through coefficients or weights that stand for the relative influence of the entry neurons on other neurons, in an analogy with the human being brain behavior. There are various types of neural networks and, among them, the feedforward networks make up one of the most utilized classes.

With no further considerations on the physical-chemical processes involved in the transmission of information among the biological neurons, the signal enters the neuron through the dendrites and next it is transmitted to other neurons of the neural network via the axon. The passage of a neuron signal to other neuron dendrites is named synapse, which basically has the function of modulating the signal exchanged through them. In the artificial neuron this signal modulation, or signal intensity, is represented by a ponderation factor, named synaptic weight.

In the feedforward network (Figure 1), the neurons are connected to all the neurons in the posterior layer. The information deriving from a layer undergoes a pondering through weights and is sent to all the neurons in the following layer.

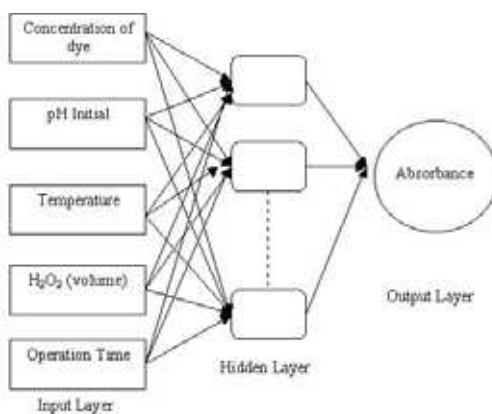


Fig. 1. Example of FeedForward Neural Network Model applied to Oxidative Advanced Process

In the feedforward networks the processing elements of a same layer work in parallel and the process among the layers is sequential.

The Equations that rule the feedforward networks are:

$$s_j^{(k)} = w_{o_j}^{(k)} + \sum_{i=1}^{N_k} w_{ij}^{(k)} x_i^{(k-1)} \quad (1)$$

$$x_j^{(k)} = f(s_j^{(k)}) \quad (2)$$

In this relation,  $s_j^{(k)}$  refers to the output of k layer i element activation function, indicates the weight pondered sum through the inputs and  $w_{ij}^{(k)}$  refers to the synaptic connections at k layer j element input, where I is the connection index and  $N_k$  is the k layer processing element number.

The feedforward neural network input and output neurons can be related by sigmoidal or linear type functions, given by Equations (3) and (4) respectively.

$$y_j = f(s_j) = \frac{1}{1 + e^{-s_j}} \quad (3)$$

$$y_j = f(s_j) = s_j \quad (4)$$

However, other transference functions can be used depending on the characteristics of the problem being studied.

The linear activating function for the output layer is adequate for continuous phenomena, as for instance the oxygen biochemical demand or the absorbance degree in decoloration process. The sigmoidal type transference functions are necessary to introduce non linearities in the network.

Training a network aims to adjust their weight in such a way that the application of a pattern produces an output value, and in this sense the Generalized Delta Rule or any other defined rule intends to reduce the network quadratic error indicated by:

$$\varepsilon = \sum_{j=1}^m (d_j - y_j)^2 \quad (5)$$

In Equation (5)  $d_j$  stands for the experimental or real value and  $y_j$  represents the value predicted from the neural model (Loesch & Sari, 1996).

From a mathematical standpoint, if a network has n processing elements in the input layer and m elements in the output layer, then the network processes the vector  $X \in \mathfrak{R}^n$ , supplying a vector  $Y \in \mathfrak{R}^m$  in such a way that the network works as a function  $f: \mathfrak{R}^n \rightarrow \mathfrak{R}^m$ . The training algorithm named backpropagation refers to the way the weights are adjusted and this algorithm is also known as Generalized Delta Rule.

In the Generalized Delta Rule, in order to minimize the mean square error the derivatives defined by Equation (6) are estimated.

$$\vec{\nabla}_j^k = \frac{\partial \varepsilon}{\partial W_j^{(k)}} \quad (6)$$

The backpropagation algorithm utilizes this derivative information (gradient) to change the weights according to Equation (7):

$$W_j^{(k)}(n+1) = W_j^{(k)}(n) + \mu \left( -\vec{\nabla}_j^k W_j^{(k)}(n) \right) \quad (7)$$

In Equation (7)  $\mu > 0$  is the network learning rate that controls the degree in which the gradient affects the weight changes and n represents the current iteration.

The neural network model adopted in this work comprises three layers: input, hidden and output. Some theorems have already been found out relative to the network characteristics:

- if a function consists of a finite collection of points, then a three layer network is able to learn it;
- in case this function is continuous and defined in a compact domain, a three layer network is able to learn it, as long as there are enough processing elements in the hidden layer.

The linear activating function for the output layer is adequate for continuous phenomena, as for instance the oxygen biochemical demand or the absorbance degree in decoloration process. The sigmoidal type transfer functions are necessary to introduce non linearities in the network.

### 3. Advanced Oxidative Process AOP

Advanced Oxidative Processes are methods for water treatment used on substances resistant to conventional processes (Quici *et al.*, 2005). Advanced Oxidative Processes are based on generation of hydroxyl radicals ( $\cdot OH$ ) have been applied to pollutant breakdown due to the radical's high oxidative power (2.8 V).

The Fenton reagent was discovered approximately 100 years ago and its use as an oxidant in the breakdown of organic compounds dates back to 1960 (Neyens & Baeyens, 2003). The Fenton reaction has the advantage of completely breaking down contaminants, producing water, carbon dioxide and non-organic salts through oxidant dissociation and hydroxyl radical production, which acts and destroys organic compounds.

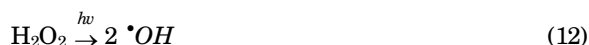
It is characterized as a mix of hydrogen peroxide and iron salts (Lu *et al.*, 2001), generating hydroxyl radicals (Equations 8 and 9):



The production of hydroxyl radical is potentially increased by the association of the ultraviolet radiation, according to the reaction given by the Equation (10), known as Photo-Fenton Process.



In this work the action of Photo-Fenton processes combined with ozone action has been studied. The beneficial effects of using ozone or oxygen peroxide in UV combined processes are highlighted as related to the individual employment of each one, as the rate of hydroxyl radicals is strongly increased. Ozone is a powerful oxidant ( $E_0=2.07$  V) which is able to react with molecules possessing non-saturated links (C=C, C=N, N=N, etc.) (Cogate & Pandit, 2004). In the presence of ultraviolet radiation, the ozone also can form the radical according to Equations (11) and (12):



## 4. Results and analysis

### 4.1 Neural approximation of the reduction of cod effluents from the manufacturing of polyesters through photo-fenton process/ozonization

For this experiment, a “Pyrex” glass reactor, 1000 mL with an ozone diffusing whirl pooling system was employed. The ultra-violet source (UV) was two 125 W mercury vapor lamps. The thermostated bath was made with a temperature controller and an ozonizer.

The reagents and solutions used were: Fenton reagent –  $\text{H}_2\text{O}_2$  at 30% v/v and  $\text{FeSO}_4 \cdot 7\text{H}_2\text{O}$  0.18 mol  $\text{L}^{-1}$ ; reagents for COD – solution of  $\text{Ag}_2\text{SO}_4$  conc (98 w/w),  $\text{K}_2\text{Cr}_2\text{O}_7$  1.0 eq  $\text{L}^{-1}$ ,  $\text{HgSO}_4$  (98 % w/w); for pH control –  $\text{NaOH}$  5.0 eq  $\text{L}^{-1}$  and  $\text{H}_2\text{SO}_4$  5.0 eq  $\text{L}^{-1}$

Iron sulphate was initially added at a concentration of 0.18 mol/L for every trial, and the oxygen peroxide concentration was of 30 % of the total weight. The generation of ozone was performed by the method of electrical discharge via dielectric barriers with the following characteristics: 220 V electrical energy, required power of 60 W, goods with oxygen or dry air, working pressure below 2 bar and production of up to 1.0 g of  $\text{O}_3$  per hour. The ozonization occurred with the use of bubbling system through diffusion, with a flow scattering adapted to its outlet. The ozone was given by the conversion of  $\text{O}_2$  to  $\text{O}_3$  through the Ozone Generator MV 01, which allows a control of variation in its flow.

Table 1 shows the minimum and maximum values of the input variables in the process.

Inlet variables	Minimum	Maximum
$T_1$	30 min	120 min
$[\text{O}_3]$	2 mg/ L	4 mg/ L
$T_2$	30 min	120 min
$V_1$	2.5 mL	15 mL
pH	2	5
T	25 °C	35 °C
$V_2$	3 mL	18 mL

Table 1. Input variables and their respective levels

All the neural models were implemented with the use of the software MatLab. The neural model input and output values were normalized in such a way that the average value would be zero and the standard deviation equal to 1. In Table 2 we can see the results

Neurons (Hidden Layer)	Training	Validation	Testing	Epochs
8	0.993	0.980	0.991	6
11	0.994	0.995	0.990	17
12	0.995	0.998	0.996	12
16	0.983	0.970	0.970	8
18	0.993	0.988	0.989	7
21	0.965	0.989	0.991	6
23	0.994	0.987	0.989	11

Table 2. Pearson Correlation Coefficients

calculated through ANN with their linear correlation coefficients, reached during the training and net generalization and verification phase. It can be noticed that the behavior of the created ANN shows an optimal performance.

During the net training process a number of configurations were made with the number of existing neurons in the hidden layer. The best results are shown in Table 3. Among them, we underline the configuration that acted with twelve neurons in the hidden layer, for that was the one that presented best results. The net incorporates 7 neurons in the input layer, corresponding to the 7 input variables; the hidden layer is built with twelve neurons and the net closes with the outcome layer, using 1 neuron referring to the output variable named COD decrease. The charts on Figures 3, 4 and 5 portray the best configuration reached, 12 neurons in the hidden layer.

In order to check the neural model, the data total set (27 samples) was divided in three sets: training (50 %) validation (25 %) and test (25 %). In Figures 2, 3 and 4 values of the x and y axis represent the decreasing percentage of the Chemical Oxygen Demand.

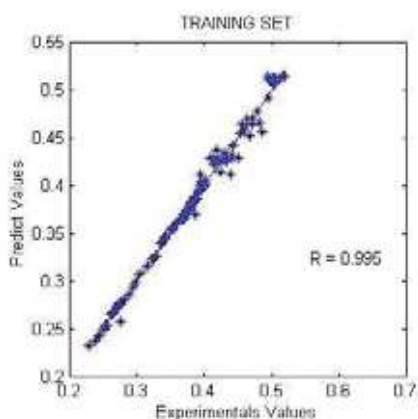


Fig. 2. Adjustment for the Training Set

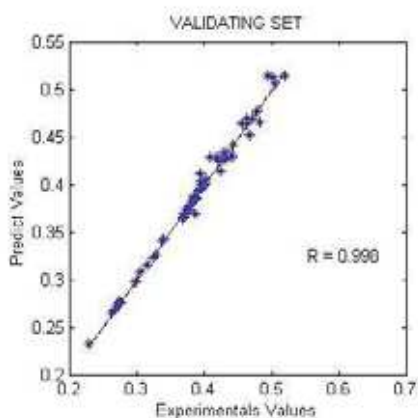


Fig. 3. Adjustment for the Validating Set

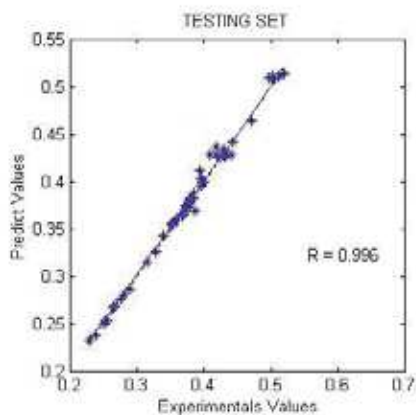


Fig. 4. Adjustment for the Testing Set

Through application of the Disturbance method (Gevrey & Lek, 2003), the relative importance of the input and output variables was evaluated (Figure 5). The Disturbance method consists of attributing isolated noises to every input variable and then observing the quadratic error determination as a function of such variation. Each input neuron passes through an error variation, and its error is compared with quadratic error, not liable to noise.

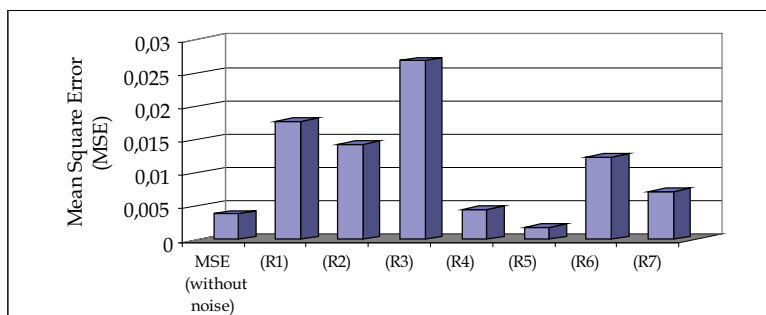


Fig. 5. Chart of MSE with input affected by noise.

We notice in the chart represented by Figure 6 that the 50 % noise provoked on each end every input neuron caused the influence perceived on the MSE value to be larger, in this order, as related to neurons: R3, R1, R2, R6, R7, R4, and R5, which represent, respectively, variables  $T_2$ ,  $T_1$ ,  $[O_3]$ ,  $T$ ,  $V_2$ ,  $V_1$  and pH. Once the disturbance method indicates only the absolute importance of each neuron or input variable, in order that the aspect of positive or negative influence could be verified, option was made for the study of the effects through Experimental Design. Thus, input variables were as well evaluated according to Experimental Design technology (27), where the most important effects can be seen in Figure 6.

Not every independent variable has a strong influence on the process of the reduction of COD as related to the observed output variable (COD), for the predominant ones, in their order, are:  $T_2$ ,  $T_1$ ,  $[O_3]$ ,  $T$  and  $V_2$ , being that the increase in  $V_1$  and pH variables caused a decrease on the yield of COD variation.



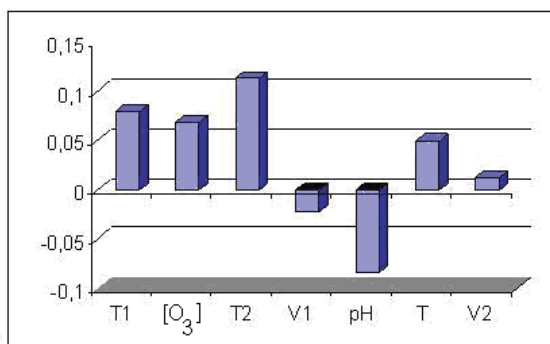


Fig. 6. Influence of Input Variables (Main Effects)

As related to V<sub>1</sub> e pH factors, a negative behavior was observed in the decrease of COD. This can be explained as a function of the fact that Fenton Reagent behaves better in a strong acid environment with a pH around 2-3. With respect and related to the increase of oxygen peroxide amount, it is observed that from a given concentration, it passes to act as a self consumer, of hydroxyl radical, according to the reaction (Equation 13):



The ozone outflow and ozonization time are important factors to be considered in the reduction of Chemical Oxygen Demand. At this point the influence of ozone for the production of hydroxyl radicals enhance, for they can combine with the  $HO_2^{\cdot}$  radical, as per the reaction (Equation 14), and thus, a greater amount of radicals is made liable to attack from organic compounds.



It is pointed out that, from a specific concentration, the hydrogen peroxide works as a hydroxyl radical self-consumer and thus a decrease of the system's oxidizing power happens.

#### 4.2 Hybrid neural model for decoloration by UV/H<sub>2</sub>O<sub>2</sub> involving process variables and structural parameters characteristics to azo dyes

Azodyes are defined as compounds that have in their structure one or more unsaturated groups -N=N- known as chromophore structure, capable of providing color through radiant energy absorbance. Azo class dyes can reach aquatic environments, dissolved or suspended in water, for the conventional treatments can not effectively remove them. The decoloration modeling process, due to the dye complex nature and its dependence on a lot of factors, brings a high level of difficulty to the problem, characterizing itself as a multiple analysis problem.

The polluted water color is reduced when there is cleavage of -C=C- and -N=N- bonds or the cleavage of the aromatic and heterocyclic rings. A lot of factors may influence the dye chromophore behavior and we have, as example, the dye feature solubility, which is influenced by the change of one substituting in the aromatic ring, with the inclusion of sulfonate groups. Hydroxyl radicals ( $\cdot OH$ ) formed in the H<sub>2</sub>O<sub>2</sub> photolysis process under

UV light action and responsible for the organic compound degradation process start, have a short lifetime, in such a way that they can react only where they are formed in a 180 Å mean distance. This reaction occurs more likely in homogeneous means.

Thus, the proposed model, which relates the azodye structure to the discoloration rate via UV/ H<sub>2</sub>O<sub>2</sub> process was set in function of the azo bond number (LA) and sulphonate group number (GS) parameters, besides the process operational parameters.

The azodyes and their properties of interest are presented in Table 3.

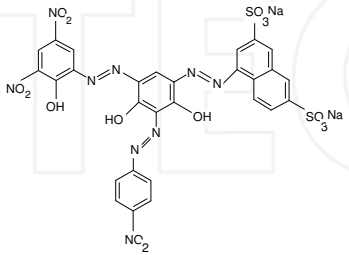
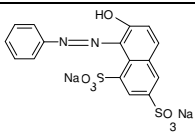
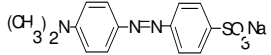
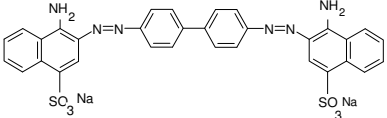
Name	$\lambda_{\max}$	Structure	LA	GS
Acid Brown 75	430		3	2
Acid Orange 10	480		1	2
Acid Orange 52	463		1	1
Direct Red 28	499		2	2

Table 3. Azodyes Characteristics

Table 4 defines the process operational variant dominium and the Table 3 also defines the dyes structural variant dominium, remarkably in discrete form, being defined by the sets GS={1,2} and LA={1,2,3}.

Parameters	min	max
Operating Time (min)	5	150
Dye Mass (mg)	100	300
H <sub>2</sub> O <sub>2</sub> (ml)	2	30
Initial pH	2	11
Temperature (°C)	22	45

Table 4. Operational variant dominium

The decoloration was evaluated in function of the absorbance, measured every 5 minutes via removal of 2 ml of sample, through the Femto 600 spectrophotometer, in the maximum wavelengths raised from the dyes in aqueous solution. The network used in this work was the feedforward backpropagation type implemented at Matlab environment and the sample total kit comprises 498 inlet-outlet values, which were initially normalized. After normalization, the kit of sample data was divided in three sets: training, validation and test for further verification of neural model generalization capacity. Figure 7 presents the network macrostructure utilized in the training process.

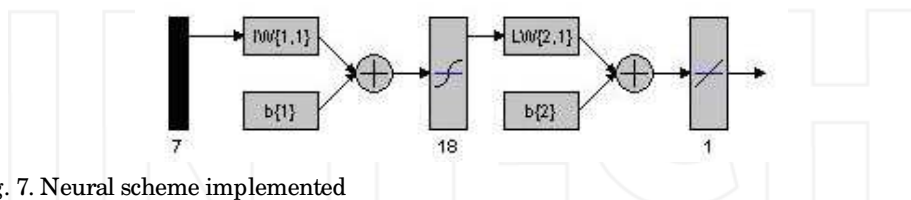


Fig. 7. Neural scheme implemented

As a general feature, in the model proposed the inlet layer is composed of seven independent variants named with azo bond number, sulphonic group number, dye concentration, reaction mean pH, time of operation of the reactor,  $H_2O_2$  volume and temperature. The outlet layer is represented by the absorbance. The hidden layer was composed by a neuron variable number, for each model, in a range from 1 to 25 Neurons, aiming to map a relation of the form  $A=f(LA, GS, Cc, pH, TO, Vp, T)$ , where A stands for the absorbance, LA is azo bond number, GS the sulphonate group number, Cc the dye concentration, TO is the photo-oxidizing process operation time, Vp is the hydrogen peroxide volume and T the reaction mean temperature.

The Pearson Correlation coefficients higher than 0.9 indicate again the good neural adjustment quality. 16 neurons in the hidden layer was the configuration chosen. Figures 9 to 12 indicate the relation between the real values (T) and the values foreseen by the neural model (A) of the absorbance values.

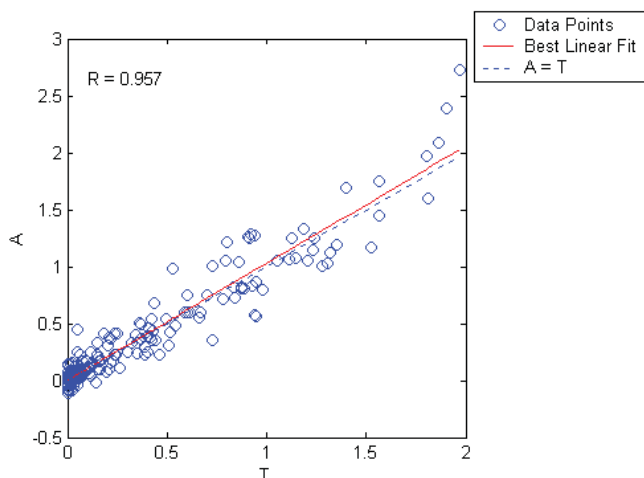


Fig. 8. Training Set Adjustment

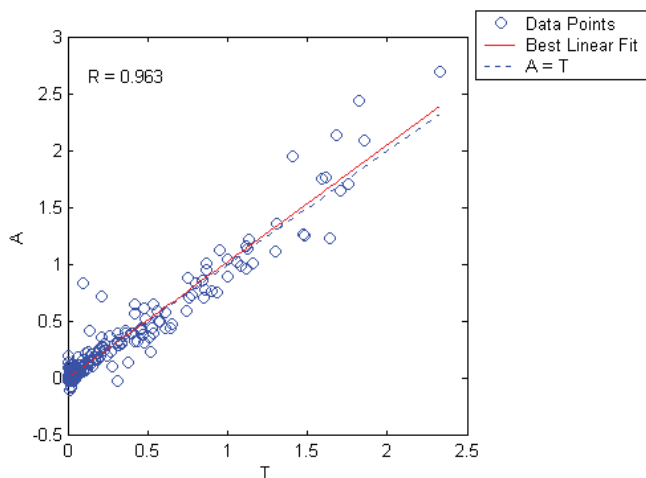


Fig. 9. Validation Set Adjustment

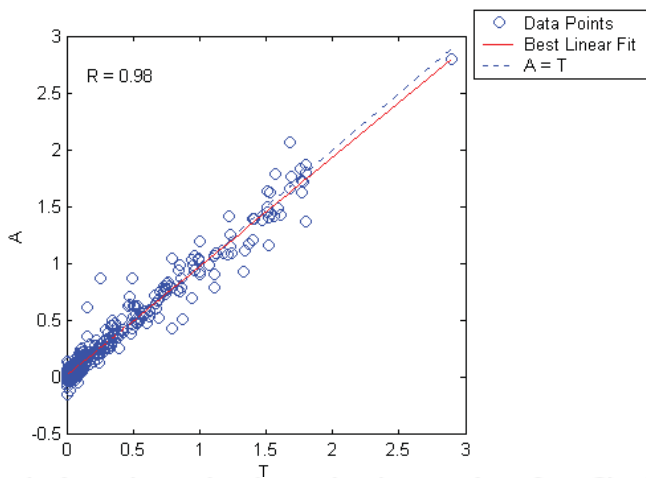


Fig. 10. Test Set Adjustment

The application of the Garson Partition Method reveals a slight predominance of the time of operation in the decoloration process and shows a balance between the structural parameters influence, that is, between the azo bonds and the suphonate groups (Table 5). The Garson method (Equation 15) and is founded in the partition of the hidden and outlet layer neural weights, in order to determine each network inlet variant relative importance (Garson, 1991), being formulated as shown:

Input Variables	Neuron	Importance (%)
Azo Bond number	1	15.48
Sulphonate group number	2	15.74
Concentration (dye)	3	15.95
Initial pH	4	13.41
Operating Time	5	16.53
H <sub>2</sub> O <sub>2</sub> (volume)	6	10.28
Temperature	7	12.61

Table 5. Classification of the Input Variables

$$I_j = \frac{\sum_{m=1}^{N^h} \left( \frac{|w_{jm}^{ih}|}{\sum_{k=1}^{N^i} |w_{km}^{ih}|} \times |w_{mn}^{h_o}| \right)}{\sum_{k=1}^{N^i} \left\{ \sum_{m=1}^{N^h} \left( \frac{|w_{km}^{ih}|}{\sum_{k=1}^{N^i} |w_{km}^{ih}|} \right) \times |w_{mn}^{h_o}| \right\}} \quad (15)$$

The relation  $I_j$  above mentioned is the relative importance of the  $j$ th input variable on output variable,  $N^i$  and  $N^h$  are the input and hidden neuron numbers, respectively and  $w$  represents the neural weights, and  $i$  and  $o$  superscripts refer to the input, hidden and output layers.  $k$ ,  $m$  and  $n$  subscripts refer respectively to the input, hidden and output layers.

### 4.3 Optimization of the AZO dyes decoloration process through neural networks: Determination of the H<sub>2</sub>O<sub>2</sub> addition critical point

In recent years, neural networks have been applied in various areas in the Chemical Engineering and, concerning the Advanced Oxidation Process it can be quoted the work of Pareek *et al.* (2002) in which it was studied the photodegrading of Spent Bayer liquor, with the use of a feedforward-type neural network. Pearson correlation coefficients above 0.99 were obtained in this work.

Slokar *et al.* (1999) utilized Kohonen type neural networks for modeling the Reactive Red 120 dye decoloration process, as a function of the use of H<sub>2</sub>O<sub>2</sub>/ UV.

The present work aimed the determination of an optimum mass relation between the initial amount of hydrogen peroxide and the amount of dye involved in the decoloration process. For the analysis of this relation, was chosen the corante Acid Brown 75, manufactured for industry BASF, widely used in the industries textile and of leathers. It is observed that works related to the degradation or discolouration of this corante had not been found in the bibliography.

The Acid Brown 75 decoloration was evaluated as a function of the absorbance measured every 5 minutes, via Femto 600 spectrophotometer, at the maximum absorbance wavelength (430 nm), optimized from the dye absorbance spectrum in aqueous solution.

The mineralization extents were determined on the basis of total organic carbon content measurements (TOC), performed by using total organic carbon analyzer; TOC- ASI 5000A, Shimadzu.

The photooxidizing process was performed in a Germetec GPJ463-1 plug-flow reactor, with low pressure radiation source of 21 W, and at the end of each experiment, the system, for washing purposes, was filled with slight acid solution and recirculated.

Table 6 defines the levels of the operational variables utilized in the experiments.

	pH	TO (min)	[dye] mg/ L	$V_{H_2O_2}$ (ml)	T (°C)
min (-1)	2	15	30	2	22
max (+1)	11	150	100	22	45

Table 6. Levels of the Operational Variables

An experimental design (2<sup>5</sup>) was implemented making up 32 experiments for the dye. The 5 minute interval data collection provided the formation of a neural network input matrix of 528 lines (samples) by 5 columns (process input variables) with the addition of some random experiments. The addition of these random points was made in central and intermediate points to the extremes of the variables. The output factor of a neural model was constituted of 528 absorbance values in the range of [0, 2].

The sample set deriving from the experiments was divided in training (50%), validation (25%) and test (25%). A scheme for implementing the optimization process by means of “complete” mapping of values simulated by the neural model can be visualized in Figure 11.

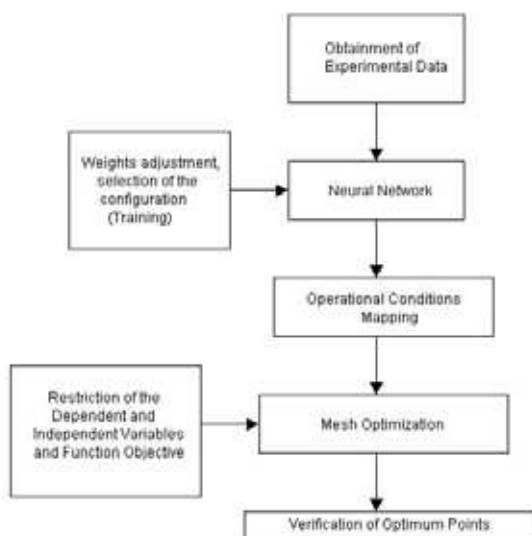


Fig. 11. Implementation of the Optimization Process

After the training and validation phases of the neural model obtained, the mapping of the operational conditions was performed. This phase comprised the discretization of all possible process inlet variables. The multifunctional points discretized and simulated by the neural model generated discretized absorbance values. The discretization period was equal to 0.01 when simulating the neural model obtained.

Once simulated the discretization process to obtain the absorbance values, the linear regression (Time of Operation versus Absorbance) was performed (least square method) for the adjustment of the constant of reaction (k) in a pseudo first order model, mapping the values of this constant through the discretization of the inlet variables, up to the obtainment of its maximum value of this constant.

The following restrictions were imposed during the training phase and complete mapping or discretization.

$$22^{\circ}C \leq T_i \leq 45^{\circ}C \quad (16)$$

$$30mg / L \leq [dye] \leq 100mg / L \quad (17)$$

$$GD = 0.90 \quad (18)$$

$$2 \leq pH \leq 11 \quad (19)$$

$$15 < TO \leq 150 \text{ mim} \quad (20)$$

$$2ml \leq V_{H_2O_2} \leq 22ml \quad (21)$$

Thus, the objective was to determine the process inlet variables values that provided the maximum value of the reaction constant, with the restriction of being reached a decoloration degree imposed as a maximum of 90% for this study.

The photooxidation is supposed to be a reaction of pseudo first order and the kinetics of color degrading can be expressed by:

$$\frac{dC_{dye}}{dt} = -kC_{dye} \quad (22)$$

The integration of this expression produces:

$$\ln(C_{dye}) = -kt + c_1 \quad (23)$$

From this expression, by linear regression, the values of the constants of reaction kinetics were determined. These values made the composition of the objective function to be mapped in a discretized form by the neural model.

Table 7 present the results of the adjustments for the training (50%), validation (25 %) and test (25 %) sets. The percentages refer to the experimental data total set.

The values of the Pearson Correlation Coefficients above 0.98 for value predicted for absorbance and absorbance real value indicate a good adjustment and prediction capacity for the neural model. The neural model obtained (16 neurons in the hidden layer) mapped a multidimensional space of the form Absorbance=( $[dye]$ , pH, T, TO,  $V_{H_2O_2}$ ).

Neurons Hidden Layer	R (training)	R (validation)	R (test)
8	0.965	0.954	0.923
12	0.976	0.971	0.963
15	0.982	0.980	0.979
16	0.987	0.981	0.984
20	0.951	0.934	0.921

Table 7. Coefficients of Correlation

The graphic verification of the H<sub>2</sub>O<sub>2</sub> addition critical behavior was performed through surface graphs. The k reaction constant maximum value was reached experimentally for values of F in the range of 50 to 60, according to the Equation (24):

$$F = \frac{m_0}{m_1} \quad (24)$$

In the Equation (24), m<sub>0</sub> represents the initial hydrogen peroxide mass and m<sub>1</sub> stands for the dye mass.

Figure 12 exemplifies the contour surface graph obtained for experimental values.

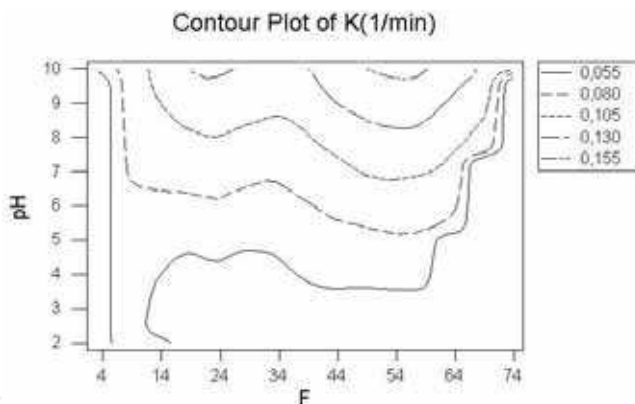
Fig. 12. Contour Surface, ABr 75, T<sub>i</sub>=45 °C, 15<TO<150

Table 8 shows some results of the pseudo first order adjustment, where the best performances of the process around a mass relation close to F=50.449 is verified.

In Table 9, some results from contour surfaces graphs (exemplified in Figure 11) are presented, for different operational conditions.

#### 4.4 Discoloration process modelling by Neural Network

Initially a high dye concentration of 170 mg/ L and a lesser amount of hydrogen peroxide (1ml) was established for a model experiment. This model experiment was performed up to the point where the absorbance came close to zero value, providing a time of 150 min, that was set as this variable amplitude range maximum value, being characterized a process inspection model. Table 10 presents the levels for which the proposed neural network input variable dominium set was established.



F	K(1/ min)	R
3.2450	0.0625	0.9989
9.9990	0.0971	0.9864
16.6650	0.1253	0.9985
26.7170	0.1296	0.9966
33.0330	0.1326	0.9912
50.4490	0.1564	0.9958
53.2216	0.1481	0.9982
56.3206	0.1386	0.9956
73.6900	0.1112	0.9975
100.0900	0.1097	0.9965

Table 8. Constant of Pseudo First Order

pH	m <sub>dye</sub>	F <sub>real</sub>	F <sub>predicted</sub>
9.8	100	50<F<60	55.55
10.0	120	50<F<60	51.33
10.5	130	50<F<60	52.22
10.1	140	50<F<60	58.00
9.9	150	50<F<60	50.00
9.6	200	50<F<60	57.89
9.4	250	50<F<60	58.90
10.0	300	50<F<60	53.76

Table 9. Some Results of the Complete Mapping

Variable Level	min	max
H <sub>2</sub> O <sub>2</sub> (ml)	2	15
[dye] (mg/ L)	3	170
pH	2	12
Temperature (°C)	21	45
Operating Time (minute)	15	150

Table 10. Variables Level

The performance of the method indicated irrelevant results in the reduction of color at absence of peroxide or radiation in isolated processes. The input variable matrixes presented to the neural model are generically shown by:

$$X = \begin{bmatrix} c_1 & pH_1 & t_1 & V_1 & T_1 \\ c_2 & pH_2 & t_2 & V_2 & T_2 \\ \cdot & \cdot & \cdot & \cdot & \cdot \\ \cdot & \cdot & \cdot & \cdot & \cdot \\ \cdot & \cdot & \cdot & \cdot & \cdot \\ c_{218} & pH_{218} & t_{218} & V_{218} & T_{218} \end{bmatrix} \quad (25)$$

Aiming to verify the existence of this matrix outliers, or solitary points of experiment, and in order to check the homogeneity of the data, each sample “leverage” (Figure 3) was estimated, which is a measurement of how the sample influences the totality of data, and a small value identifies little sample influence over the model building.

Ferreira et al. (1999) indicate that a critical value, or practical rule for the identification of anomalous points, namely, considered points with “leverage” higher than  $3k/n$ , where  $n$  is the number of samples (218) and  $k$  the number of main components or latent variables, five of them (analysis of components in Matlab environment) for the current work, resulting in a critical value of 0.068807 and, therefore, some samples were discarded from the set to be tested. Matlab `prepcap` (`pn, 0.02`) code transforms the input set data matrix already normalized (`pn`), retaining only the components that contribute with more than 2% in the input data set variance.

There are several methods for picking out the sets to be used as training, validation and test sets. Kanduc *et al.* (2003) establish the random selection, Kennard-Stone and Kohonen maps as some of the possibilities to be employed.

In the present work, the data were worked by following the basic algorithm given by:

1. A clustering was established using K-Means algorithm.
2. After having determined the groups, a statistic test was used to set the training validation and test groups, in such a way that the training, validation and test sets pattern deviation and mean value be equal to less than a value tending to zero.
3. The input variables (in number of 5) and the output variables were processed in such a way that the mean value for each vector containing the dependent and independent variables be zero and the pattern deviation equal to 1, through the `pn = (p-meanp)/ stdp` Matlab environment algorithm, where `p` is the input or output process matrix or data vector. In Matlab environment, this normalization and the generated set recording were performed by the command:

```
%NORMALIZED SET GENERATION
```

```
[pn, meanp, stdp, tn, meant, stdt] = prestd(p', t');
```

The implementation of algorithm K-Means identified 4 clusters, herein named as clusters 1 to 4 (Table 11):

Cluster	Cluster samples number
1	57
2	58
3	51
4	52

Table 11. Cluster Distribution

Table 12 presents the best results with a single hidden layer topology, with the respective linear (R) correlation coefficients. Neural networks with a hidden layer and a sufficiently large number of neurons can interpret any input-output structure and that the hidden layer neuron number is determined in function of the required accuracy.

All the configurations worked with the same 0.01 learning tax and the training performed in 22 epochs.

The functions used in the network training algorithm were `tansig` and `purelin` (Matlab language) and the network weight actualization function was the Levenberg-Marquardt backpropagation (`trainlm` in Matlab language).

Hidden layer neuron number	R <sub>1</sub> (Training Set)	R <sub>2</sub> ( Validation set)	R <sub>3</sub> (Test Set)
8	0.988	0.982	0.979
12	0.976	0.971	0.963
15	0.990	0.980	0.979
16	0.991	0.986	0.981
20	0.990	0.984	0.977

Table 12. Correlation Coefficients

The function of error performance was MSE, or mean square error, and the performance learning function utilized was the descending Gradient (learngdm).

Some of the parameters can be visualized in the sequence of commands given by:

```
net=newff(minmax(pn),[co 1{'tansig','purelin'}], 'trainml');
net.trainParam.epochs = 100; net.trainParam.goal = 0;
net.trainParam.lr = 0.01; % Learning tax
net.trainParam.show = 25; net.trainParam.mc = 0.9;
net.trainParam.lr_inc = 1.05; net.trainParam.lr_dec = 0.7; net.trainParam.max_perf_inc = 1.04;
net.performFcn='MSE';
```

The diagram of the network implemented may be seen in Figure 13, where 5 input layer neurons related to the 5 network input variables, the 16 layer hidden layer and the input layer with a neuron corresponding to the absorbance output variable.

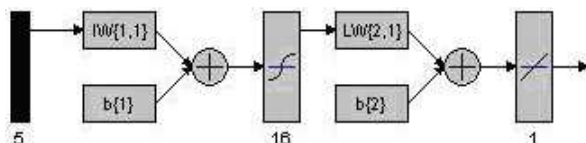


Fig. 13. Diagram of implemented Neural Model

The linear activating function for the output layer is adequate for continuous phenomena, as for instance the oxygen biochemical demand or the absorbance degree in DISCOLORATION process. The sigmoidal type transference functions are necessary to introduce non linearities in the network.

In order to prevent overfitting problem, the training is interrupted if the error for the validation set becomes bigger than the training set error.

In function of the results obtained, hidden layer 16 neuron configuration was chosen. Graphically, the results may be visualized via Figures 14 through 16.

The level of influence of each input variable concerning the modeling problem output variable may be obtained through the neural weight matrix.

As it can be seen in the Table 13, all independent variables strongly influence the absorbances of the discoloration process.

In order to confirm the value importance order classification the perturbation method was applied. Gevrey *et al.* (2003) indicates the perturbation method for input variable analysis. This consists of changes in the form  $x_i = x_i + \delta$ , where  $x_i$  is the selected input variable and  $\delta$  is the variable change or noise. The method consists of attributing this noise and verifying the changes in the output  $y_i$  variable. In this work, the mean square error was used as comparison criterion.

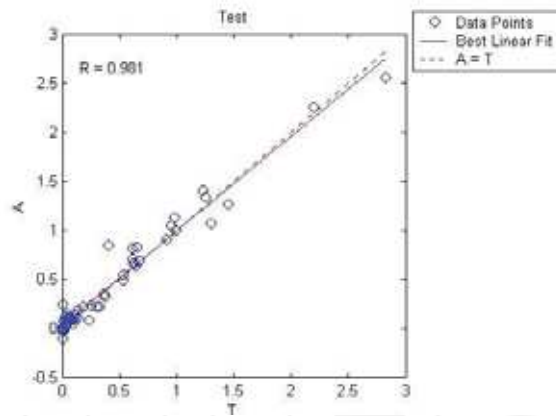


Fig. 14. Linear Regression Test Set

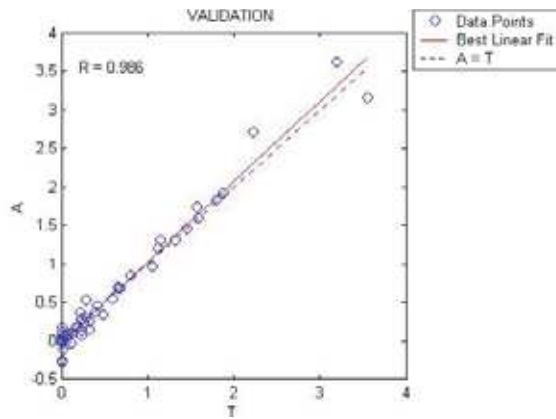


Fig. 15. Linear Regression for validation set

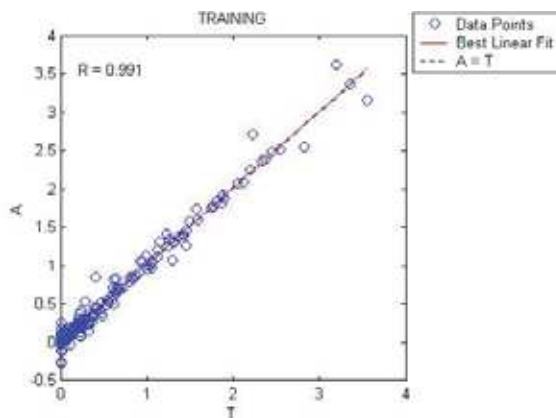


Fig. 16. Linear Regression for Training Set

Variable	Importance(%)
H <sub>2</sub> O <sub>2</sub>	19.15
[dye]	21.44
pH	21.49
Temperature	16.97
Operating Time	29.95

Table 13. Input Variable Classification

The value  $\delta = 10\%$  attributed in each variable, maintaining the other constants, produced the graph shown in Figure 17, where the major importance of time of operation (t) is visualized, followed by the reaction mean (pH) and hydrogen peroxide volume (V).

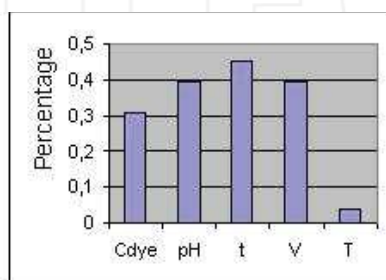


Fig. 17. MSE Variation Percentage

The factors that presented the minor MSE importance were the dye concentration ( $C_{dye}$ ) and temperature (T), keeping this order of importance. It is noticed the coincidence in the three most important factors in the Garson Partition and Pertubation Methods, namely, time of operation, pH and hydrogen peroxide volume.

In order to verify the stability of the values obtained through Garson Partition and Pertubation methods, the network trainings were repeated 10 times and the average contribution of each variable was calculated.

By comparing the results obtained through Garson Partition and Pertubation methods, an inversion is noticed concerning the dye concentration and temperature variables behavior, but equivalence was observed in the other variables, maintained the levels of importance.

A 10% noise value is attributed to the input data matrix aiming to verify the network capacity to self-adapt and prevent small failures or measurement errors, and Table 14 shows the network adaptation capacity to these noises, with the mean quadratic errors, and the linear correlation coefficients for training set ( $R_1$ ), validation set ( $R_2$ ) and test set ( $R_3$ ).

	$R_1$	$R_2$	$R_3$
Noise (0)%	0.978	0.977	0.947
Noise(10%)	0.974	0.968	0.923

Table 14. Correlation Coefficients under noise in the input variables

## 5. Conclusion

The employment of a neural model to describe the photo-chemical influence of effluents from polyesters and alcolic resins has shown excellent results, as the model can describe the complex behavior of the process within the experimentation range employed.

The model achieved also allows, for the study of the influence of input variables in the photo-chemical process.

Thus, simulations based on neural nets afford the estimation of the complex behavior of oxidation processes that combine photo-Fenton and ozone agents. Such information is essential for the treatment of industry effluents.

Concerning the efficiency of the oxidizing process utilized, it has to be pointed out the obtainment of the best results close to 55%, values that due to high Chemical Oxygen Demand initial value present the practical feasibility of the oxidizing method proposed for effluents with very high organic charge values.

In relation to case B, This work proposes, via neural networks, a model that involves the process operational and compound structure features to be treated, in such a way that a higher model amplitude occurs. This process has the advantage of working as a database, where new samples, with totally different characteristics, may be added with the need of equationing a new model. Implemented the neural model and analyzed the correlation coefficients (approximately 0.96 for the data total, validation and test sets) it was verified the good model prediction capacity and also the possibility of determining the inlet variable influence degree of the Garson Method. The neural model, because it simply involves the numerical or statistical "behavior analysis", does not troubles about the mathematics involved in the process and, thus, it makes possible the analysis of structural sets that comprise variants of several different spectrums, such as operational and structural ones, opening room for a hybrid and more embracing model. It is pointed out the capacity of application of the herein named hybrid modeling by neural networks, with the possible incorporation of other structural parameters which may foresee different environment values such as oxygen chemical, dissolved organic carbon demand, among other factors of environmental concern. In the present model, the neural model hybrid character was not connected to the fact that the entry variant values be experimental or deriving from certain mathematics models but in these variant nature composition aspect, being of the process operational aspect and structural concerning the dyes. For dyes with the same azo bonds number and sulfonated groups other characteristics, as label hydrogen number, benzenic and naphthalenic can be incorporated, which will object of further researches.

In relation to the Case "C", The implementation of a neural model and the optimization through complete mapping of the dominium of the independent variables in a process of decoloration by UV/ H<sub>2</sub>O<sub>2</sub> is presented as a promising technique in the optimization of processes with multiple inlet variables.

The neural model reached good prediction capacity with Pearson Correlation Coefficients above 0.98 for the training, validation and test sets.

From this neural model, the discretization of all process variables could be performed, which made possible the search for the Acid Brown 75 dye decoloration process critical point through the use of UV/ H<sub>2</sub>O<sub>2</sub>. The determination of the critical point, or maximum amount of Hydrogen Peroxide to be added as a function of the dye initial mass, was established in a 50<F<60 interval, coinciding with the real values obtained in the experiments.

The study of the case “An Acid Orange 52 dye DISCOLORATION neural model”, with hydrogen peroxide, activated by UV radiation, was evaluated concerning five factors. The neural network was trained with 218 samples and utilized a configuration with a hidden layer and 16 neurons in this layer, presenting high correlation coefficients for training, validation and test sets (>0.98), verifying the network prediction capacity with high accuracy level. The input layer is formed by five variables: dye concentration, initial pH, time of operation, hydrogen peroxide volume at 30% and temperature. The study of the variable influence level determined that the input variables that influence the Acid Orange 52 DISCOLORATION process are time of operation, initial pH and hydrogen peroxide volume. However, temperature and concentration of the dye should not be neglected, as they also appear to be significant factors.

## 6. References

- Ferreira, M. C. M., Antunes, A.M., Melgo, M.S., Volpe, P.L., Chemometrics I: multivaried calibration, a Tutorial, Química Nova, vol. 22, 1999
- Garson, G.D., AI Expert, p.46, 1991;
- Gevrey, M., Dimopoulos I., Lek, S., Review and comparison of methods to study the contribution of variables in artificial neural networks models, Ecological Modelling 160, 249-264, 2003.
- Gogate, P. R. e Pandit, A. B. A review of imperative technologies for wastewater treatment I: oxidation technologies at ambient conditions, Advances in Environmental Research 8, 501 –551, 2004.
- Kanduc, R. K., Zupan, J., Madcen, N., Separation of data on the training and test for modelling: a case study for modelling of five colour properties of a white pigment, Chemometrics and Intelligent Laboratory Systems 65, p. 221-229, 2003;
- Loesch C., Sari, S. T., Redes Neurais Artificiais Fundamentos e Modelos, Editora da Furb, 1996;
- Lu, M.C., Lin, C.J, Liao, C.H., Ting, W.P., Huang, R.Y. *Influence of pH on the dewatering of activated sludge by Fenton's reagent*, Wat. Sci. Technol. 44, 327-332, 2001.
- Neyens, E. e Baeyens, J A review of classic Fenton's peroxidation as an advanced oxidation technique, Journal of Hazardous Materials B98, 33-50, 2003.
- Pareek, V. K., Brungs, M. P., Adesina, A. A., Sharma, R. (2002) Artificial neural network modeling of a multiphase photodegradation system. Journal of Photochemistry and Photobiology A: Chemistry 149, 139-146;
- Quici, N., Morgada, M. E., Piperata, G., Babay, P., Gettar, R. T., Litter, M. I. Oxalic acid destruction at high concentrations by combined heterogeneous photocatalysis and photo-Fenton processes, Catalysis Today, 2005.
- Slokar, Y.M., Zupan, J, Marechal, A. M. (1999) The use of artificial neural network (ANN) for modeling of the H<sub>2</sub>O<sub>2</sub>/ UV decoloration process: part I. Dyes and Pigments 42, 123-135;



## **Artificial Neural Networks - Application**

Edited by Dr. Chi Leung Patrick Hui

ISBN 978-953-307-188-6

Hard cover, 586 pages

**Publisher** InTech

**Published online** 11, April, 2011

**Published in print edition** April, 2011

This book covers 27 articles in the applications of artificial neural networks (ANN) in various disciplines which includes business, chemical technology, computing, engineering, environmental science, science and nanotechnology. They modeled the ANN with verification in different areas. They demonstrated that the ANN is very useful model and the ANN could be applied in problem solving and machine learning. This book is suitable for all professionals and scientists in understanding how ANN is applied in various areas.

### **How to reference**

In order to correctly reference this scholarly work, feel free to copy and paste the following:

Messias Borges Silva, Oswaldo Luiz Cobra Guimarães, Adriano Francisco Siqueira, Hécio José Izário Filho, Darcy Nunes Villela Filho, Henrique Otávio Queiroz de Aquino, Ivy dos Santos Oliveira and Carlos Roberto de Oliveira Almeida (2011). Applications of Neural Networks in Advanced Oxidative Process, Artificial Neural Networks - Application, Dr. Chi Leung Patrick Hui (Ed.), ISBN: 978-953-307-188-6, InTech, Available from: <http://www.intechopen.com/books/artificial-neural-networks-application/applications-of-neural-networks-in-advanced-oxidative-process>

# **INTECH**

open science | open minds

### **InTech Europe**

University Campus STeP Ri  
Slavka Krautzeka 83/A  
51000 Rijeka, Croatia  
Phone: +385 (51) 770 447  
Fax: +385 (51) 686 166  
[www.intechopen.com](http://www.intechopen.com)

### **InTech China**

Unit 405, Office Block, Hotel Equatorial Shanghai  
No.65, Yan An Road (West), Shanghai, 200040, China  
中国上海市延安西路65号上海国际贵都大饭店办公楼405单元  
Phone: +86-21-62489820  
Fax: +86-21-62489821